analysis of variance (ANOVA). The statistical significance of differences in other data between two administration groups was calculated with the Student's *t*-test. All data were calculated with StatView® Software, version 5 (ABACUS Concepts, Berkeley, CA). A value of $P<0.05$ was considered statistically significant.

RESULTS

Preparation and characterisation of CDDP-incorporating polymeric micelles (NC-6004)

Cisplatin-incorporating polymeric micelles (NC-6004) consist of CDDP and PEG–P(Glu) (Figure 1A). Furthermore, NC-6004 consists of PEG, a hydrophilic chain which constitutes the outer shell of the micelles, and the coordinate complex of P(Glu) and CDDP, a polymer–metal complex-forming chain which constitutes the inner core of the micelles. The molecular weight of PEG–P(Glu) as a sodium salt was approximately 18 000 (PEG: 12 000; P(Glu): 6000). The CDDP-incorporated polymeric micelles were clearly discriminated from typical micelles from amphiphilic block copolymers. The driving force of the formation of the CDDP-incorporated micelles is the ligand substitution of Pt(II) atom from chloride to carboxylate in the side chain of P(Glu). The molar ratio of CDDP to the carboxyl groups in the copolymers was 0.71 (Nishiyama *et al*, 2003). A narrowly distributed size of polymeric micelles (30 nm) was confirmed by the DLS measurement

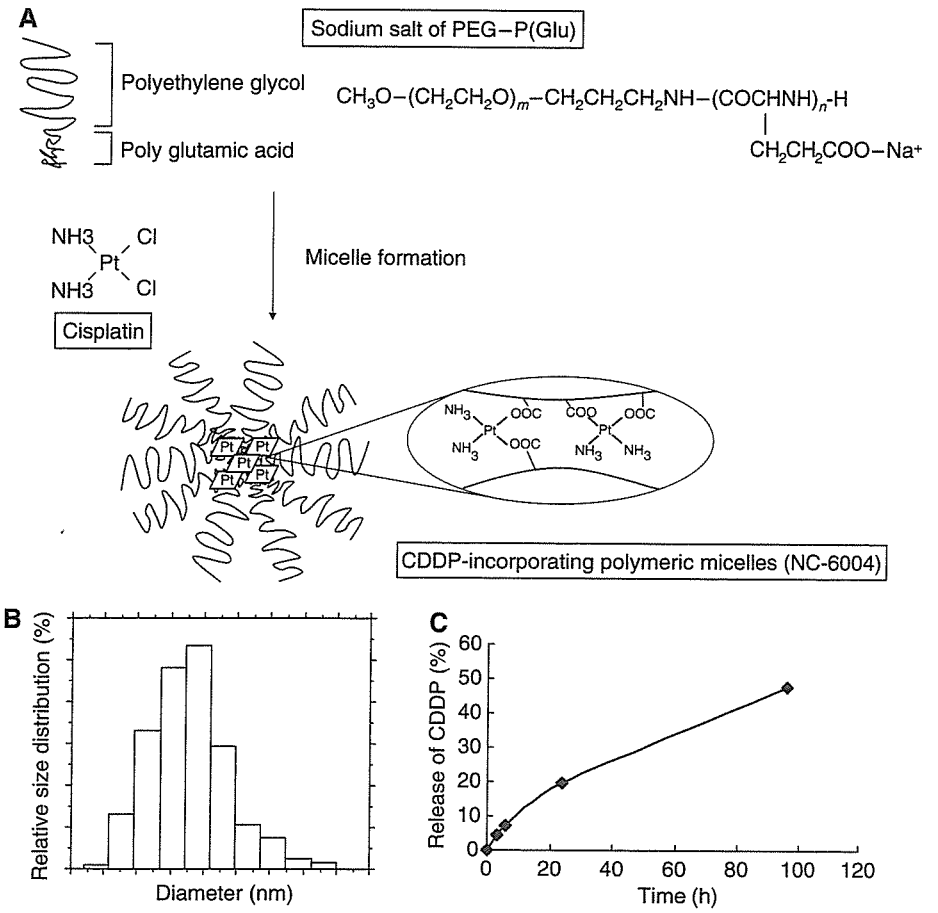

Figure 1 Preparation and characterisation of CDDP-incorporating polymeric micelles (NC-6004). (**A**) Chemical structures of CDDP and PEG–P(Glu) block copolymers, and the micellar structures of CDDP-incorporating polymeric micelles (NC-6004). (**B**) The particle size distribution of NC-6004 measured by the dynamic light-scattering method. The mean particle size of NC-6004 was approximately 30 nm. (**C**) Release of CDDP from NC-6004 in saline at 37°C.

Table 1 Pharmacokinetic parameter estimates for CDDP and NC-6004 in rats (see text for definitions of parameters)

Compound	Rat	T_{max}[a] (h)	C_{max}[a] ($\mu g\,ml^{-1}$)	$t_{1/2z}$ (h)	AUC_{0-t} ($\mu g\,h\,ml^{-1}$)	$AUC_{0-inf.}$ ($\mu g\,h\,ml^{-1}$)	CL_{tot} ($ml\,h^{-1}\,kg^{-1}$)	$MRT_{0-inf.}$ (h)	V_{ss} ($l\,kg^{-1}$)
CDDP	Mean	0.083	11.67	34.50	20.47	75.73	70.67	46.57	3.00
	s.d.		0.57	16.14	2.25	26.13	20.34	22.38	0.61
NC-6004	Mean	0.50	89.90	6.43	1325.90	1335.47	3.77	10.67	0.04
	s.d.		4.29	0.55	77.85	75.99	0.21	0.15	0.0023

The pharmacokinetic parameters were calculated after fitting to a noncompartment model using WinNonlin program. [a]For CDDP group, T_{max} represents time of maximum concentration.

(Figure 1B). Also, the static light scattering (SLS) measurement revealed that the CDDP-loaded micelles showed no dissociation upon dilution and the CMC was less than 5×10^{-7}, suggesting remarkable stability compared with typical micelles from amphiphilic block copolymers (Nishiyama *et al.* 1999). It is assumed that the interpolymer crosslinking by Pt(II) atom might contribute to stabilisation of the micellar structure.

The release rates of CDDP from NC-6004 were 19.6 and 47.8% at 24 and 96 h, respectively (Figure 1C). Therefore, the release of CDDP was as slow as the previously reported release (Nishiyama *et al*, 2003). In distilled water, furthermore, NC-6004 was stable without releasing CDDP (data not shown).

Pharmacokinetics and pharmacodynamics

Frameless atomic absorption spectrophotometry could measure serum concentrations of Pt up to 48 h after i.v. injection of NC-6004, but could measure them only up to 4 h after i.v. injection of CDDP. NC-6004 showed a very long blood retention profile as compared with CDDP. The AUC_{0-t} and C_{max} values were significantly higher in animals given NC-6004 than in animals given CDDP, namely, 65- and 8-fold, respectively ($P<0.001$ and 0.001, respectively) (Table 1, Figure 2A). Furthermore, the CL_{tot} and V_{ss} values were significantly lower in animals given NC-6004 than in animals given CDDP, that is, one-nineteenth and one-seventy-fifth, respectively ($P<0.01$ and 0.01, respectively) (Table 1).

Regarding the concentration–time profile of Pt in various tissues after i.v. injection of CDDP or NC-6004, all organs measured exhibited the highest concentrations of Pt within 1 h after administration in all animals given CDDP (Figure 2B). Furthermore, animals given NC-6004 exhibited the highest tissue concentrations of Pt in the liver and spleen at late time points (24 and 48 h after administration, respectively). However, the concentrations decreased on day 7 after administration (Figure 2C). In addition, and in a similar manner to other drugs which are incorporated in polymeric carriers, NC-6004 demonstrated accumulation in organs of the reticuloendothelial system, for example, liver and spleen. At 48 h after administration, tissue concentrations of Pt in the liver and spleen were 4.6- and 24.4-fold higher for NC-6004 than for CDDP. On the other hand, a marked increase in tissue Pt concentration was observed immediately after administration in the kidneys of animals given CDDP. Renal Pt concentration at 10 min and 1 h after administration were 11.6- and 3.1-fold lower, respectively, in animals given NC-6004 than in animals given CDDP. Furthermore, the maximum concentration (C_{max}) in the kidney was 3.8-fold lower at the time of NC-6004 administration than at the time of CDDP administration.

Regarding the tumour accumulation of Pt, tumour concentrations of Pt peaked at 10 min after administration of CDDP. On the other hand, tumour concentrations of Pt peaked at 48 h after administration of NC-6004 (Figure 2D). The maximum concentration (C_{max}) in tumour was 2.5-fold higher for NC-6004 than for CDDP ($P<0.001$). Furthermore, the tumour AUC was 3.6-fold higher for NC-6004 than for CDDP (81.2 and 22.6 $\mu g\,ml\,h^{-1}$ in animals given NC-6004 and CDDP, respectively).

In vitro cytotoxicity

NC-6004 was tasted on 12 human tumour cell lines derived from bladder, colon, lung, gastric, and breast cancers. The IC_{50} values of NC-6004 were 6-to 15-fold higher than those of CDDP (Table 2).

In vivo antitumour activity

BALB/*c* nude mice implanted with a human gastric cancer cell line MKN-45 showed decreased tumour growth rates after i.v. injection of CDDP and NC-6004 (Figure 3A). In the administration of CDDP,

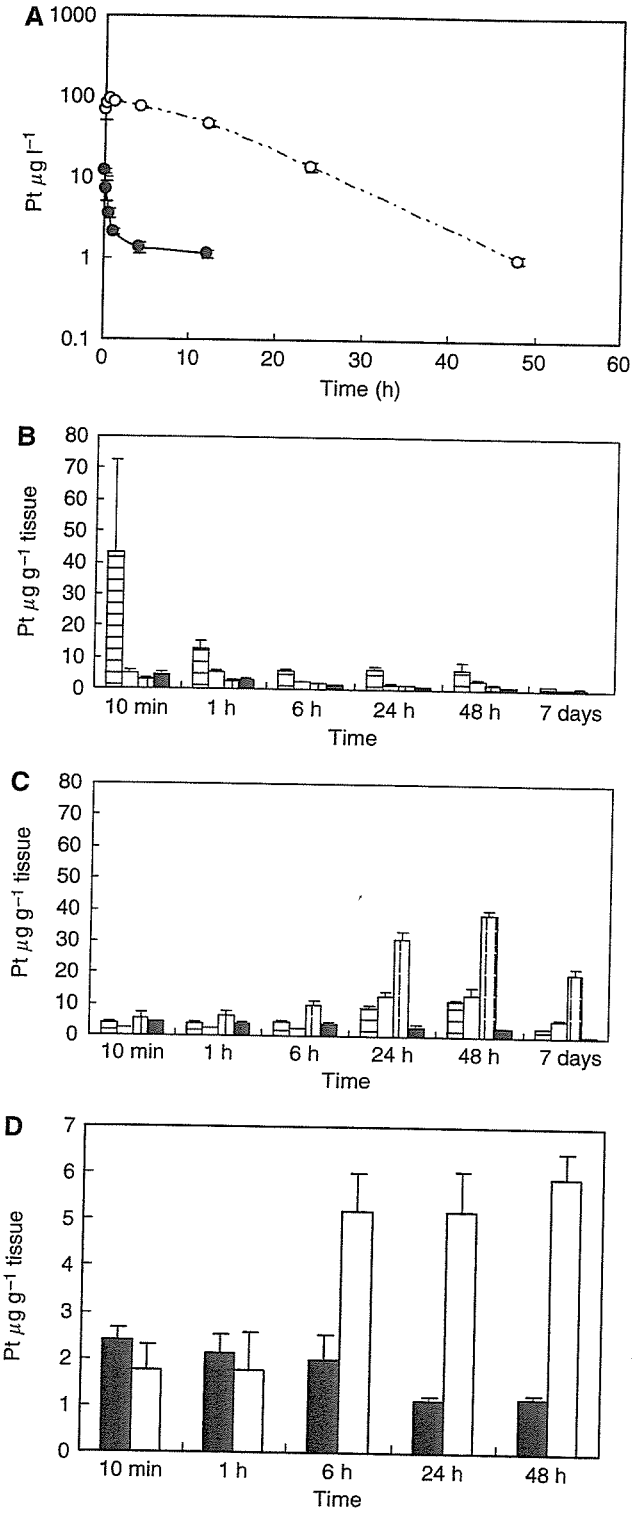

Figure 2 Time profiles of Pt concentration in the plasma and tissue distribution of Pt after a single i.v. injection of CDDP (5 mg kg^{-1}) or NC-6004 (an equivalent dose of 5 mg kg^{-1} CDDP). (**A**) Concentration–time profile of Pt in the plasma after a single i.v. injection of CDDP (●) and NC-6004 (○) in rats ($n=3$). Tissue distribution of Pt after a single i.v. injection of CDDP (**B**) and NC-6004 (**C**) in rats ($n=3$) (kidney (▤), liver (□), spleen (▥), and lung (■)). (**D**) Time profiles of Pt concentration in the MKN-45 solid tumour after a single i.v. injection of CDDP (■) and NC-6004 (□) in MKN-45 bearing BALB/*c* nude mice ($n=3$). Values are expressed as the mean ± s.d.

Table 2 IC_{50} values(μM) of CDDP and NC-6004 in various cancer cell lines

		Exposure time (h)			
		48		72	
Cancer	**Cell line**	**CDDP**	**NC-6004**	**CDDP**	**NC-6004**
Bladder cancer	EJ-1	2.46	25.45	1.86	18.44
	J82	2.78	42.89	2.42	20.27
	MBT-2	15.88	>100	5.67	71.67
Colon cancer	Colo201	34.77	>100	28.52	>100
	Colo320	16.32	>100	9.71	81.15
	HT-29	14.44	>100	8.83	>100
Lung cancer	A549	21.43	>100	20	>100
	EBC-1	>100	>100	9.36	84.78
	PC-14	16.81	>100	8.73	87.11
Gastric cancer	MKN-28	>100	>100	8.23	76.81
	MKN-45	7.12	68.36	6.94	43.81
Breast cancer	MCF-7	12.78	>100	5.71	54.71

the CDDP 5 mg kg^{-1} administration group showed a significant decrease ($P<0.01$) in tumour growth rate as compared with the control group. In the administration of NC-6004, NC-6004 2.5 mg kg^{-1} administration group ($P<0.05$) and 5 mg kg^{-1} administration group ($P<0.01$) showed significant decreases in tumour growth rate as compared with the control group. However, the NC-6004 administration groups at the same dose levels as CDDP showed no significant difference in tumour growth rate. The same animal model was used to repeat the study using the drugs at different dose levels, and similar tendencies were observed (data not shown). Regarding time-course changes in body weight change rate, the CDDP 5 mg kg^{-1} administration group showed a significant decrease ($P<0.001$) in body weight as compared with the control group. On the other hand, none of the NC-6004 administration groups showed a decrease in body weight as compared with the control group (Figure 3B).

Nephrotoxicity and hepatotoxicity of CDDP and NC-6004

In the CDDP 10 mg kg^{-1} administration group, four of 12 animals died from toxicity within 7 days after drug administration. No deaths occurred in the NC-6004 10 mg kg^{-1} administration group and the NC-6004 15 mg kg^{-1} administration group. Regarding renal function, the BUN concentrations on day 7 after the administration of 5% glucose, CDDP 10 mg kg^{-1}, NC-6004 10 mg kg^{-1}, and NC-6004 15 mg kg^{-1} were 20.8 ± 3.0, 65.3 ± 44.4, 20 ± 4.5, and 24.6 ± 18.2 mg dl^{-1}, respectively. The plasma concentrations of creatinine on day 7 after the administration of 5% glucose, CDDP 10 mg kg^{-1}, NC-6004 10 mg kg^{-1}, and NC-6004 15 mg kg^{-1} were 0.27 ± 0.03, 0.68 ± 0.23, 0.28 ± 0.04, and 0.45 ± 0.11 mg dl^{-1}, respectively. The CDDP 10 mg kg^{-1} administration group showed significantly higher plasma concentrations of BUN and creatinine as compared with the control group ($P<0.05$ and 0.001, respectively), with the NC-6004 10 mg kg^{-1} administration group ($P<0.05$ and 0.001, respectively), and also with the NC-6004 15 mg kg^{-1} administration group ($P<0.05$ and 0.05, respectively) (Figure 4A and B). Light microscopy indicated tubular dilation with flattening of the lining cells of the tubular epithelium in the kidney from all animals in the CDDP 10 mg kg^{-1} administration group. On the other hand, no histopathological change was observed in the kidneys from all animals in the NC-6004 10 mg kg^{-1} administration group (Figure 4C and D). Regarding hepatic function, the plasma concentrations of GOT on day 7 after the administration of 5% glucose, CDDP 10 mg kg^{-1}, NC-6004 10 mg kg^{-1}, and NC-6004 15 mg kg^{-1} were 68 ± 6.8, 65.1 ± 5.5, 106 ± 13.1, and 97 ± 16.2 IU l^{-1}, respectively. The plasma

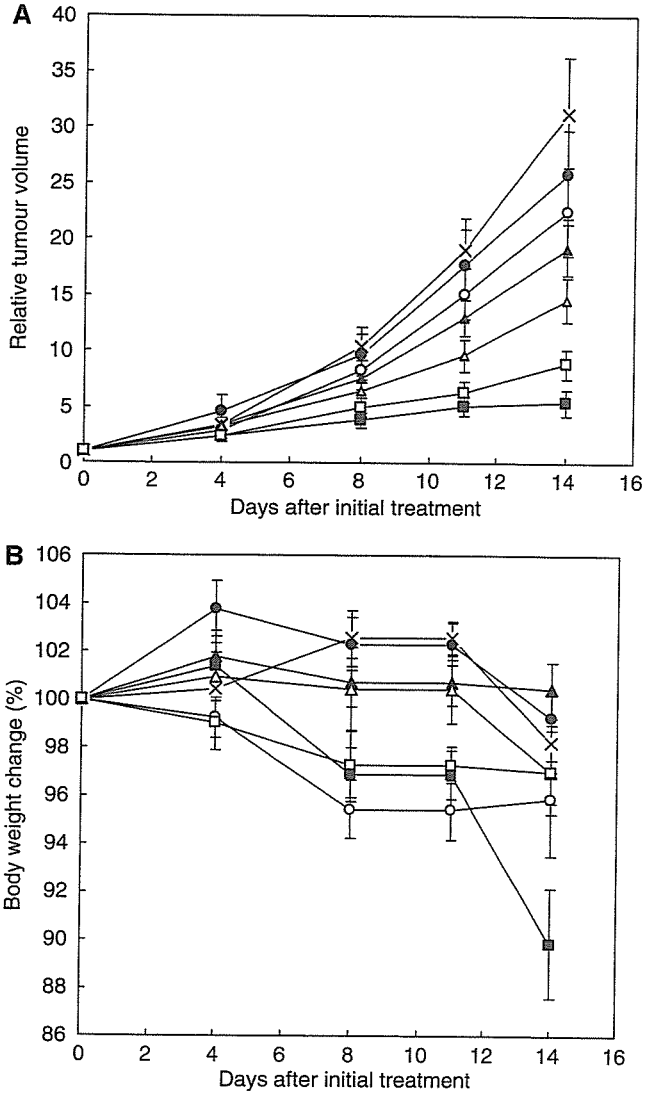

Figure 3 Relative changes in MKN-45 tumour growth rates in nude mice. (**A**) Cisplatin and NC-6004 were injected i.v. every 3 days, three administrations in total, at CDDP-equivalent doses of 0.5 mg kg^{-1} (●, ○), 2.5 mg kg^{-1} (▲, △), and 5 mg kg^{-1} (■, □), respectively. Glucose (5%) was injected in the control mice (×). (**B**) Changes in relative body weight. Data were derived from the same mice as those used in the present study. Values are expressed as the mean ± s.e.

concentrations of GPT on day 7 after the administration of 5% glucose, CDDP 10 mg kg^{-1}, NC-6004 10 mg kg^{-1}, and NC-6004 15 mg kg^{-1} were 39.6 ± 10, 32 ± 6.4, 92 ± 18.9, and 55 ± 11.3 IU l^{-1}, respectively. The CDDP 10 mg kg^{-1} administration group showed plasma concentrations of GOT and GPT which were comparable to those in the control group. However, the NC-6004 10 mg kg^{-1} administration group, which presented the same dose level as the CDDP 10 mg kg^{-1} administration group, showed significantly higher plasma concentrations of GOT and GPT ($P<0.001$ and 0.01, respectively) as compared with the control group. Furthermore, the NC-6004 15 mg kg^{-1} administration group also showed significantly higher plasma concentrations of GOT ($P<0.001$) as compared with the control group. However, the plasma concentrations of GOT and GPT on day 14 after the administration of NC-6004 10 mg kg^{-1} were comparable to those in the control group (74 ± 2.3 and 42.8 ± 5.1 IU l^{-1}, respectively) (Figure 4E). These results lead to the conjecture that rats which were given NC-6004 10 mg kg^{-1}, i.v., showed transient and reversible hepatotoxicity.

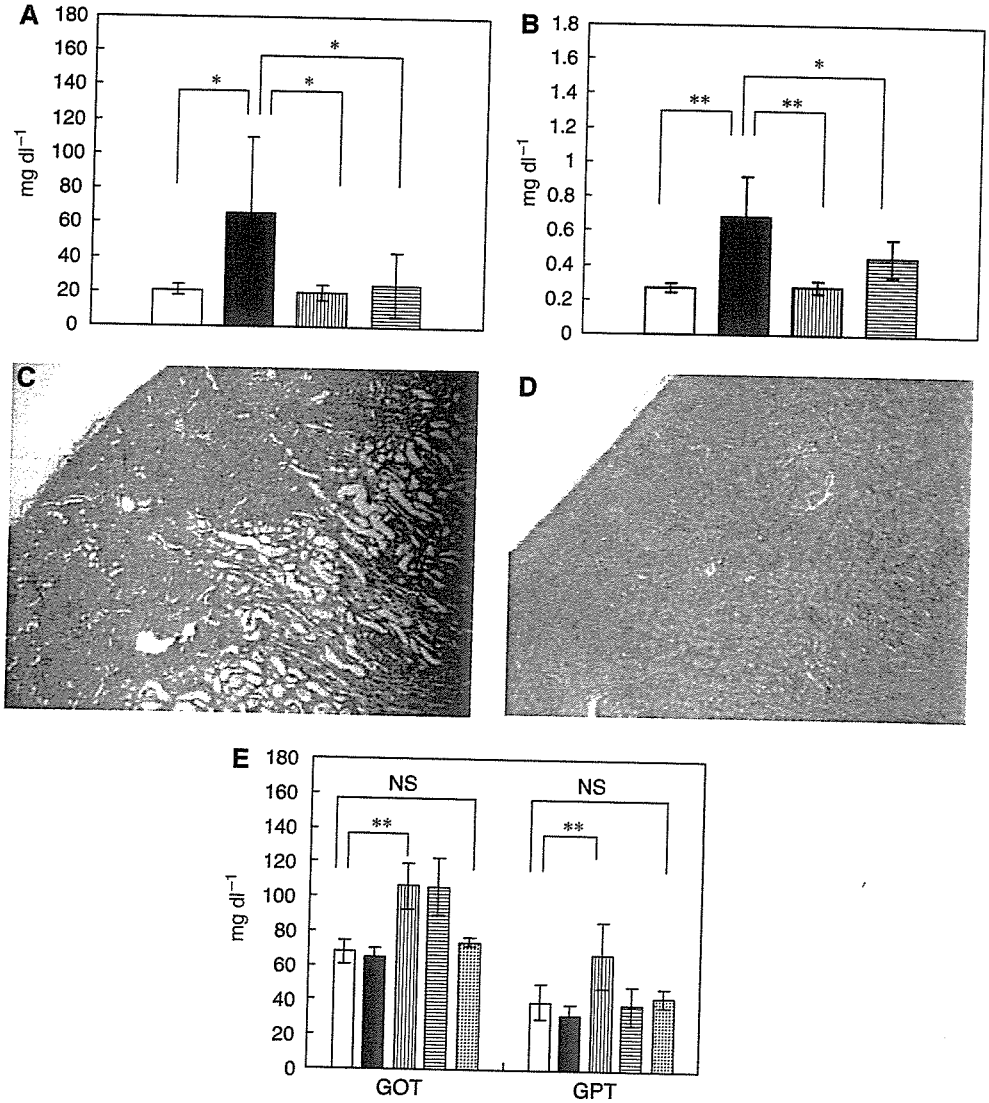

Figure 4 Nephrotoxicity and hepatotoxicity of CDDP and NC-6004. Plasma concentrations of BUN (**A**) and creatinine (**B**) were measured after a single i.v. injection of 5% glucose (□) ($n=8$), CDDP at a dose of 10 mg kg^{-1} (■) ($n=12$), NC-6004 at a dose of 10 mg kg^{-1} ($n=13$) on a CDDP basis (▥), and at a dose of 15 mg kg^{-1} on a CDDP basis (▤) ($n=8$) to rats. Histopathological changes in the kidney on day 7 after the i.v. injection of CDDP (**C**, ×4) and NC-6004 (**D**, ×4) in rats at an equivalent dose of 10 mg kg^{-1} CDDP. In rats given CDDP, widespread tubular degeneration as indicated by tubular dilation with flattening of the lining cells of tubular epithelium was seen. On the other hand, no histopathological change was observed in the kidney from all animals in the NC-6004 10 mg kg^{-1} administration group. For hepatotoxicity (**E**), the plasma concentrations of GOT and GPT were measured on day 7 after administration. When administering NC-6004 at a dose of 10 mg kg^{-1} on a CDDP basis, five of 13 blood samples were taken on day 14 after administration (▦). The other samples were taken on day 7 administration. In the group given CDDP at a dose of 10 mg kg^{-1}, four of 12 rats died within 7 days. Values are expressed as the mean ± s.d. *$P<0.05$, **$P<0.001$, NS: not significant.

Neurotoxicity of CDDP and NC-6004

Neurophysiological examination revealed that MNCVs in animals given 5% glucose, CDDP, and NC-6004 were 44.2 ± 3.5, 40.94 ± 5.08, and 40.62 ± 0.63 m s^{-1}, respectively. No significant difference was found among the groups with respect to MNCV. Furthermore, SNCVs in animals given 5% glucose, CDDP, and NC-6004 were 42.86 ± 8.07, 35.48 ± 4.91, and 43.74 ± 5.3 m s^{-1}, respectively. Animals given NC-6004 showed no delay in SNCV as compared with animals given 5% glucose. On the other hand, animals given CDDP showed a significant delay ($P<0.05$) in SNCV as compared with animals given NC-6004 (Figure 5A). In addition, histopathological examination with electron microscopy revealed degenerations, as manifested by electron photomicrographs indicating degenerative changes, for example, loss of microtubules, degeneration in the cytoplasm of Schwann cells, loss of filaments, and an irregular inner loop, in approximately 80% of myelinated segments of the sciatic nerve from animals given CDDP. On the other hand, animals given NC-6004 exhibited nearly normal electron photomicrographs of the sciatic nerve as the control animals did (Figure 5B and C). These results indicate that NC-6004 reduced peripheral neurotoxicity as compared with CDDP. Furthermore, regarding body weight change as an indication of general toxicity, furthermore, the NC-6004 administration groups showed significant inhibition of body weight decrease ($P<0.001$) as compared with the CDDP administration group ($P<0.001$) (Figure 5D).

The analysis by ICP-MS on sciatic nerve concentrations of Pt could not detect Pt in the sciatic nerve from animals given 5% glucose (data not shown). Sciatic nerve concentrations of Pt in

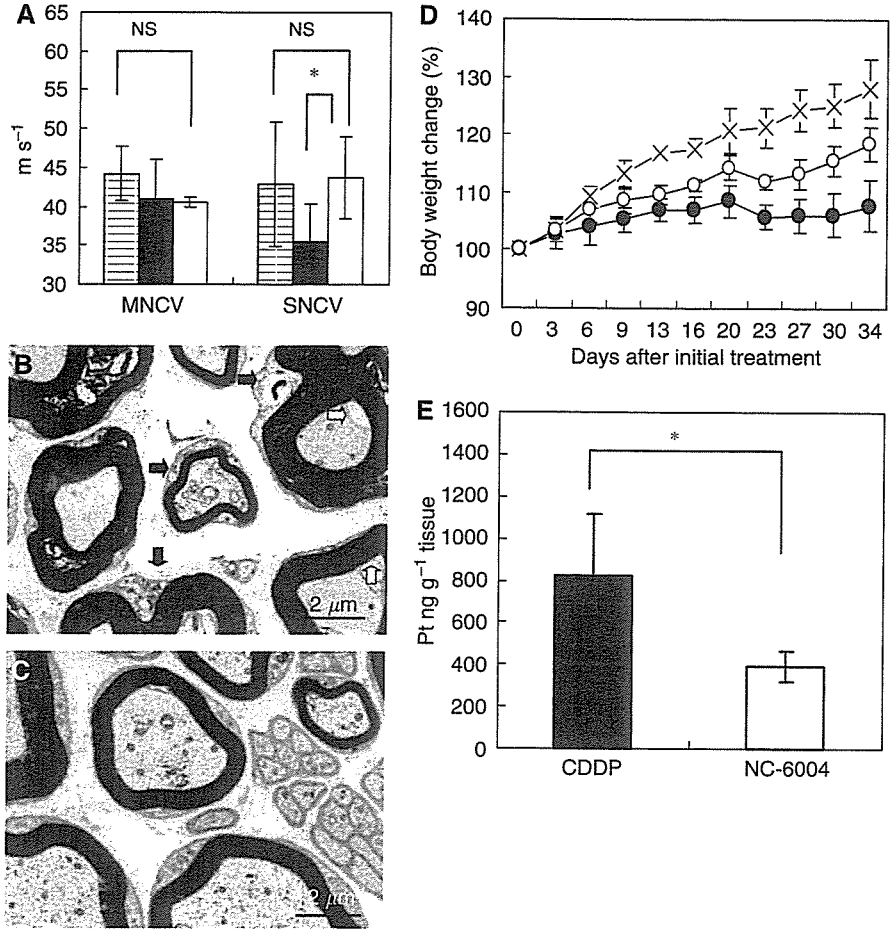

Figure 5 Neurotoxicity of CDDP and NC-6004 in rats. Rats ($n=5$) were given CDDP (2 mg kg^{-1}), NC-6004 (an equivalent dose of 2 mg kg^{-1} CDDP), or 5% glucose, all i.v. twice a week, 11 administrations in total. (**A**) Sensory nerve conduction velocity and MNCV of the sciatic nerve at week 6 after the initial administration (control (⊟), CDDP (●), and NC-6004 (□)). Histopathological changes of the sciatic nerve were examined by electron microscopy after the administration of CDDP (**B**) and NC-6004 (**C**). In rats given CDDP, widespread degenerations as indicated by loss of microtubules, loss of filaments, degeneration in the cytoplasm of Schwann cells (➡), and an irregular inner loop (⇨) were seen. On the other hand, animals given NC-6004 exhibited nearly normal electron micrographs of the sciatic nerve as the control animals. (**D**) Changes in relative body weight. Data were derived from the same rats as those used in the present study (control (×), CDDP (●), and NC-6004 (○)). (**E**) The Pt concentration in the sciatic nerve. Rats were given CDDP (■) (5 mg kg^{-1}, $n=5$), NC-6004 (□) (an equivalent dose of 5 mg kg^{-1} CDDP, $n=5$), or 5% glucose ($n=2$), all i.v. twice a week, four administrations in total. On day 3 after the final administration, a segment of the sciatic nerve was removed and the Pt concentration in the sciatic nerve was measured by ICP-MS. Body weight changes are expressed as the mean ± s.e. The other data are expressed as the mean ± s.d. *$P<0.05$, **$P<0.001$, NS: not significant.

animals given CDDP and NC-6004 were 827.2 ± 291.3 and 395.5 ± 73.1 ng g^{-1} tissue. Therefore, the concentrations were significantly ($P<0.05$) lower in animals given NC-6004 (Figure 5E). This finding is believed to be a factor which reduced neurotoxicity following NC-6004 administration as compared with the CDDP administration.

DISCUSSION

The present study indicated that CDDP-incorporating polymeric micelles (NC-6004) are stable nanoparticles with a long blood retention profile as compared with free CDDP. NC-6004 showed 6- to 15-fold less potent *in vitro* cytotoxic activity in several human cancer cell lines as compared with CDDP. These findings are considered attributable to the slow release of free CDDP in the presence of abundant chloride ions because NC-6004 contains coordination bonds between the atoms of Pt(II) of CDDP and the carboxylic group in the side chain of P(Glu). *In vivo*, however, in contrast to the *in vitro* findings, NC-6004 was found to markedly reduce nephrotoxicity and neurotoxicity – dose-limiting factors of CDDP, while preserving antitumour activity, which was equivalent to or better than that of free CDDP.

Nephrotoxicity of CDDP is considered to depend on the peak urinary CDDP concentration and on the maximum CDDP concentration in the uriniferous tubules (Levi *et al*, 1982). We consider that the reduced nephrotoxicity of NC-6004 may be explained by the following facts: (1) the tendency of micelles to be less prone to filtration by nephrons because of the NC-6004 particle size (approximately 30 nm), and (2) the much lower C_{max} value for CDDP at least in the uriniferous tubules than the value following CDDP administration. NC-6004 possibly facilitates treatment on an outpatient basis because it allows safer administration to patients with decreased renal function and requires no massive fluid replacement to protect renal tissue after the administration of CDDP.

The main neuropathy of CDDP is sensory peripheral neuropathy (van der Hoop *et al*, 1990; Gregg *et al*, 1992). A delay in SNCV due to the injury of dorsal root ganglia and peripheral nerve has previously been reported in rats given CDDP, although MNCV was

preserved in the tail and hind paws of rats (McKeage *et al*, 1994; Tredici *et al*, 1998; Meijer *et al*, 1999; Tredici *et al*, 1999). Furthermore, histopathological examination revealed degenerative changes in the sciatic nerve in similar experimental animals (Cavaletti *et al*, 1992; Tredici *et al*, 1999). In the present study, animals given NC-6004 showed no delay in the SNCV, while animals given CDDP showed a significant delay in the SNCV as compared with animals given NC-6004. Neuropathologically, neuronal degeneration, which was observed following CDDP administration, was not observed with NC-6004 administration. This result is considered attributable principally to the fact that the peripheral nerve concentration of Pt decreased to half or less following NC-6004 administration than with CDDP administration. The nervous tissue concentration of Pt at the time of NC-6004 administration decreased significantly despite the fact that the plasma AUC at the time of NC-6004 administration was high, being 65-fold higher than the plasma AUC concentration with CDDP administration. We consider that this result is attributed to the marked inhibition of Pt distribution into nervous tissue in the NC-6004 administration groups as manifested by V_{ss} of 3.00 ± 0.61 and $0.04 \pm 0.0023\,l\,kg^{-1}$ in the CDDP and NC-6004 groups, respectively. In any event, we believe that the neurotoxicity of CDDP reduced by NC-6004 allows its long-term administration.

On the other hand, transient hepatic dysfunction was observed in rats. This observation indicates the proneness of Pt to accumulate in the RES of the liver because NC-6004 is, after all, said and done, a macromolecule, although preserving a stealth effect through its outer shell of PEG. We consider that caution should be exercised against hepatic dysfunction in conducting a clinical trial of NC-6004 in the future. However, the accumulation of Pt was lower following NC-6004 administration due to a decrease in V_{ss} in other organs including nerve. As shown by changes in body weight in multiple dose studies in rats, the NC-6004 administration groups have been demonstrated to show a smaller decrease in body weight as compared with the CDDP administration groups. In single-dose studies, furthermore, one dose of CDDP $10\,mg\,kg^{-1}$ was equivalent to the 50% of the lethal dose. In fact, four of 12 animals died within 7 days after administration. However, none of the eight animals in the NC-6004 group died after the administration of NC-6004 at a CDDP equivalent dose of $15\,mg\,kg^{-1}$. In terms of haematological toxicity, there was no significant difference between the CDDP and NC-6004 groups in rats (data not shown).

In murine tumour strains, CDDP-incorporating polymeric micelles showed significantly high antitumour activity (Nishiyama *et al*, 2003). In the human gastric cancer strain used in the present study, however, no significant difference was found between the NC-6004 and CDDP administration groups. A significant difference was found in antitumour activity between the NC-6004 low-dose group ($2.5\,mg\,kg^{-1}$ administration group) and the control group, while no significant difference was found between the CDDP low-dose group ($2.5\,mg\,kg^{-1}$ administration group) and the control group. Results available to date and the results from the present study lead to the consideration that the incorporation of CDDP into polymeric micelles does not reduce its antitumour activity.

Data from the present study warrant the clinical evaluation of NC-6004. We consider that the protocol for the Phase I clinical trial of NC-6004 should employ a regimen without massive i.v. drip infusion.

ACKNOWLEDGEMENTS

This work is supported by Grants-in-Aid from the Ministry of Health, Labour and Welfare of Japan. We thank Drs T Kawaguchi and K Shimada for their expert technical assistance and Mrs K Shiina for her secretarial assistance.

REFERENCES

Allen TM (1994) Long-circulating (sterically stabilized) liposomes for targeted drug delivery. *Trends Pharmacol Sci* **15:** 215–220

Bellmunt J, Ribas A, Eres N, Albanell J, Almanza C, Bermejo B, Sole LA, Baselga J (1997) Carboplatin-based *versus* cisplatin-based chemotherapy in the treatment of surgically incurable advanced bladder carcinoma. *Cancer* **80:** 1966–1972

Boulikas T, Vougiouka M (2004) Recent clinical trials using cisplatin, carboplatin and their combination chemotherapy drugs (review). *Oncol Rep* **11:** 559–595

Cassidy J, Tabernero J, Twelves C, Brunet R, Butts C, Conroy T, Debraud F, Figer A, Grossmann J, Sawada N, Schoffski P, Sobrero A, Van Cutsem E, Diaz-Rubio E (2004) XELOX (capecitabine plus oxaliplatin): active first-line therapy for patients with metastatic colorectal cancer. *J Clin Oncol* **22:** 2084–2091

Cavaletti G, Tredici G, Marmiroli P, Petruccioli MG, Barajon I, Fabbrica D (1992) Morphometric study of the sensory neuron and peripheral nerve changes induced by chronic cisplatin (DDP) administration in rats. *Acta Neuropathol (Berl)* **84:** 364–371

Cleare MJ, Hydes PC, Malerbi BW, Watkins DM (1978) Anti-tumor platinum complexes: relationships between chemical properties and activity. *Biochimie* **60:** 835–850

du Bois A, Luck HJ, Meier W, Adams HP, Mobus V, Costa S, Bauknecht T, Richter B, Warm M, Schroder W, Olbricht S, Nitz U, Jackisch C, Emons G, Wagner U, Kuhn W, Pfisterer J (2003) A randomized clinical trial of cisplatin/paclitaxel *versus* carboplatin/paclitaxel as first-line treatment of ovarian cancer. *J Natl Cancer Inst* **95:** 1320–1329

Gabizon A, Chemla M, Tzemach D, Horowitz AT, Goren D (1996) Liposome longevity and stability in circulation: effects on the *in vivo* delivery to tumors and therapeutic efficacy of encapsulated anthracyclines. *J Drug Target* **3:** 391–398

Gregg RW, Molepo JM, Monpetit VJ, Mikael NZ, Redmond D, Gadia M, Stewart DJ (1992) Cisplatin neurotoxicity: the relationship between dosage, time, and platinum concentration in neurologic tissues, and morphologic evidence of toxicity. *J Clin Oncol* **10:** 795–803

Hamaguchi T, Matsumura Y, Suzuki M, Shimizu K, Goda R, Nakamura I, Nakatomi I, Yokoyama M, Kataoka K, Kakizoe T (2005) NK105, a paclitaxel-incorporating micellar nanoparticle formulation, can extend *in vivo* antitumour activity and reduce the neurotoxicity of paclitaxel. *Br J Cancer* **92:** 1240–1246

Horwich A, Sleijfer DT, Fossa SD, Kaye SB, Oliver RT, Cullen MH, Mead GM, de Wit R, de Mulder PH, Dearnaley DP, Cook PA, Sylvester RJ, Stenning SP (1997) Randomized trial of bleomycin, etoposide, and cisplatin compared with bleomycin, etoposide, and carboplatin in good-prognosis metastatic nonseminomatous germ cell cancer: a Multiinstitutional Medical Research Council/European Organization for Research and Treatment of Cancer Trial. *J Clin Oncol* **15:** 1844–1852

Klibanov AL, Maruyama K, Beckerleg AM, Torchilin VP, Huang L (1991) Activity of amphipathic poly(ethylene glycol) 5000 to prolong the circulation time of liposomes depends on the liposome size and is unfavorable for immunoliposome binding to target. *Biochim Biophys Acta* **1062:** 142–148

Klibanov AL, Maruyama K, Torchilin VP, Huang L (1990) Amphipathic polyethylene glycols effectively prolong the circulation time of liposomes. *FEBS Lett* **268:** 235–237

Lasic DD (1996) Doxorubicin in sterically stabilized liposomes. *Nature* **380:** 561–562

Levi FA, Hrushesky WJ, Halberg F, Langevin TR, Haus E, Kennedy BJ (1982) Lethal nephrotoxicity and hematologic toxicity of *cis*-diammine-dichloroplatinum ameliorated by optimal circadian timing and hydration. *Eur J Cancer Clin Oncol* **18:** 471–477

Maeda H (2001) The enhanced permeability and retention (EPR) effect in tumor vasculature: the key role of tumor-selective macromolecular drug targeting. *Adv Enzyme Regul* **41:** 189–207

Maeda H, Matsumura Y (1989) Tumoritropic and lymphotropic principles of macromolecular drugs. *Crit Rev Ther Drug Carrier Syst* **6:** 193–210

Maeda H, Wu J, Sawa T, Matsumura Y, Hori K (2000) Tumor vascular permeability and the EPR effect in macromolecular therapeutics: a review. *J Control Rel* **65:** 271–284

Matsumura Y, Hamaguchi T, Ura T, Muro K, Yamada Y, Shimada Y, Shirao K, Okusaka T, Ueno H, Ikeda M, Watanabe N (2004) Phase I clinical trial and pharmacokinetic evaluation of NK911, a micelle-encapsulated doxorubicin. *Br J Cancer* **91:** 1775–1781

Matsumura Y, Maeda H (1986) A new concept for macromolecular therapeutics in cancer chemotherapy: mechanism of tumoritropic accumulation of proteins and the antitumor agent smancs. *Cancer Res* **46:** 6387–6392

McKeage MJ, Boxall FE, Jones M, Harrap KR (1994) Lack of neurotoxicity of oral bisacetatoammine dichlorocyclohexylamine-platinum(IV) in comparison to cisplatin and tetraplatin in the rat. *Cancer Res* **54:** 629–631

Meijer C, de Vries EG, Marmiroli P, Tredici G, Frattola L, Cavaletti G (1999) Cisplatin-induced DNA-platination in experimental dorsal root ganglia neuronopathy. *Neurotoxicology* **20**(6): 883–887

Nishiyama N, Kataoka K (2001) Preparation and characterization of size-controlled polymeric micelle containing *cis*-dichlorodiammineplatinum(II) in the core. *J Control Rel* **74:** 83–94

Nishiyama N, Kato Y, Sugiyama Y, Kataoka K (2001) Cisplatin-loaded polymer–metal complex micelle with time-modulated decaying property as a novel drug delivery system. *Pharm Res* **18:** 1035–1041

Nishiyama N, Okazaki S, Cabral H, Miyamoto M, Kato Y, Sugiyama Y, Nishio K, Matsumura Y, Kataoka K (2003) Novel cisplatin-incorporated polymeric micelles can eradicate solid tumors in mice. *Cancer Res* **63:** 8977–8983

Nishiyama N, Yokoyama M, Aoyagi T, Okano T, Sakurai Y, Kataoka K (1999) Preparation and characterization of self-assembled polymer–metal complex micelle from *cis*-dichlorodiammineplatinum(II) and poly(ethylene glycol)-poly(α,β-aspartic acid) block copolymer in an aqueous medium. *Langmuir* **15:** 377–383

Orditura M, Quaglia F, Morgillo F, Martinelli E, Lieto E, De Rosa G, Comunale D, Diadema MR, Ciardiello F, Catalano G, De Vita F (2004) Pegylated liposomal doxorubicin: pharmacologic and clinical evidence of potent antitumor activity with reduced anthracycline-induced cardiotoxicity (review). *Oncol Rep* **12:** 549–556

Pinzani V, Bressolle F, Haug IJ, Galtier M, Blayac JP, Balmes P (1994) Cisplatin-induced renal toxicity and toxicity-modulating strategies: a review. *Cancer Chemother Pharmacol* **35:** 1–9

Roth BJ (1996) Chemotherapy for advanced bladder cancer. *Semin Oncol* **23:** 633–644

Screnci D, McKeage MJ, Galettis P, Hambley TW, Palmer BD, Baguley BC (2000) Relationships between hydrophobicity, reactivity, accumulation and peripheral nerve toxicity of a series of platinum drugs. *Br J Cancer* **82:** 966–972

Tredici G, Braga M, Nicolini G, Miloso M, Marmiroli P, Schenone A, Nobbio L, Frattola L, Cavaletti G (1999) Effect of recombinant human nerve growth factor on cisplatin neurotoxicity in rats. *Exp Neurol* **159:** 551–558

Tredici G, Tredici S, Fabbrica D, Minoia C, Cavaletti G (1998) Experimental cisplatin neuronopathy in rats and the effect of retinoic acid administration. *J Neurooncol* **36:** 31–40

van der Hoop RG, van der Burg ME, ten Bokkel Huinink WW, van Houwelingen C, Neijt JP (1990) Incidence of neuropathy in 395 patients with ovarian cancer treated with or without cisplatin. *Cancer* **66:** 1697–1702

UKCCCR, PO Box 123, Kincolin's Inn Fields, London, WC2A 3PX (1998) United Kingdom Co-ordinating Committee on Cancer Research (UKCCCR) guidelines for the welfare of animals in experimental neoplasia (second edition). *Br J Cancer* **77:** 1–10

Yokoyama M, Miyauchi M, Yamada N, Okano T, Sakurai Y, Kataoka K, Inoue S (1990) Characterization and anticancer activity of the micelle-forming polymeric anticancer drug adriamycin-conjugated poly(ethylene glycol)-poly(aspartic acid) block copolymer. *Cancer Res* **50:** 1693–1700

Yokoyama M, Okano T, Sakurai Y, Ekimoto H, Shibazaki C, Kataoka K (1991) Toxicity and antitumor activity against solid tumors of micelle-forming polymeric anticancer drug and its extremely long circulation in blood. *Cancer Res* **51:** 3229–3236

Yokoyama M, Okano T, Sakurai Y, Fukushima S, Okamoto K, Kataoka K (1999) Selective delivery of adriamycin to a solid tumor using a polymeric micelle carrier system. *J Drug Target* **7:** 171–186

Acta Urol. Jpn. 51 : 651-658, 2005

TRANSRECTAL HIGH-INTENSITY FOCUSED ULTRASOUND IN THE TREATMENT OF LOCALIZED PROSTATE CANCER : A MULTICENTER STUDY

Toyoaki Uchida
The Department of Urology, Tokai University Hachioji Hospital
Shiro Baba, Akira Irie and Shigehiro Soh
The Department of Urology, Kitasato University
Naoya Masumori and Taiji Tsukamoto
The Department of Urology, Sapporo Medical University
Hiroomi Nakatsu
The Department of Urology, Asahi General Hospital
Hiroyuki Fujimoto and Tadao Kakizoe
The Department of Urology, National Cancer Center
Takeshi Ueda and Tomohiko Ichikawa
The Department of Urology, Chiba University
Nobutaka Ohta and Tadaichi Kitamura
The Department of Urology, Tokyo University
Makoto Sumitomo and Masamichi Hayakawa
The Department of Urology, National Defense Medical College
Teiichiro Aoyagi and Masaaki Tachibana
The Department of Urology, Tokyo Medical University
Ryusuke Ikeda and Kohji Suzuki
The Department of Urology, Kanazawa Medical University
Nobuo Tsuru, Kazuo Suzuki and Seiichiro Ozono
The Department of Urology, Hamamatsu University School of Medicine
Kiyohide Fujimoto, Yoshihiko Hirao
The Department of Urology, Nara Medical University
Kohichi Monden, Yasutomo Nasu and Hiromi Kumon
The Department of Urology, Okayama University
Kazuhiko Nishi and Shoichi Ueda
The Department of Urology, Kumamoto University
Hirofumi Koga and Seiji Naitoh
The Department of Urology, Kyusyu University

TRANSRECTAL HIGH-INTENSITY FOCUSED ULTRASOUND IN THE TREATMENT OF LOCALIZED PROSTATE CANCER: A MULTICENTER STUDY

Toyoaki UCHIDA[1], Shiro BABA[2], Akira IRIE[2], Shigehiro SOH[2], Naoya MASUMORI[3], Taiji TSUKAMOTO[3], Hiroomi NAKATSU[4], Hiroyuki FUJIMOTO[5], Tadao KAKIZOE[5], Takeshi UEDA[6], Tomohiko ICHIKAWA[6], Nobutaka OHTA[7], Tadaichi KITAMURA[7], Makoto SUMITOMO[8], Masamichi HAYAKAWA[8], Teiichiro AOYAGI[9], Masaaki TACHIBANA[9], Ryusuke IKEDA[10], Kohji SUZUKI[10], Nobuo TSURU[11], Kazuo SUZUKI[11], Seiichiro OZONO[11], Kiyohide FUJIMOTO[12], Yoshihiko HIRAO[12], Kohichi MONDEN[13], Yasutomo NASU[13], Hiromi KUMON[13], Kazuhiko NISHI[14], Shoichi UEDA[14], Hirofumi KOGA[15] and Seiji NAITOH[15]

[1]*The Department of Urology, Tokai University Hachioji Hospital*
[2]*The Department of Urology, Kitasato University*
[3]*The Department of Urology, Sapporo Medical University*
[4]*The Department of Urology, Asahi General Hospital*
[5]*The Department of Urology, National Cancer Center*
[6]*The Department of Urology, Chiba University*
[7]*The Department of Urology, Tokyo University*
[8]*The Department of Urology, National Defense Medical College*
[9]*The Department of Urology, Tokyo Medical University*
[10]*The Department of Urology, Kanazawa Medical University*
[11]*The Department of Urology, Hamamatsu University School of Medicine*
[12]*The Department of Urology, Nara Medical University*
[13]*The Department of Urology, Okayama University*
[14]*The Department of Urology, Kumamoto University*
[15]*The Department of Urology, Kyusyu University*

We report a multicenter trial with transrectal high-intensity focused ultrasound (HIFU) in the treatment of localized prostate cancer. A total of 72 consecutive patients with stage T1c-2N0M0 prostate cancer were treated using the Sonablate 500™ HIFU device (Focus Surgery, Indianapolis, USA). Biochemical recurrence was defined according to the criteria recommended by the American Society for Therapeutic Radiology and Oncology Consensus Panel. The median age and prostate specific antigen (PSA) level were 72 years and 8.10 ng/ml, respectively. The median follow-up period for all patients was 14.0 months. Biochemical disease-free survival rates in all patients at 1 and 2 years were 78% and 76%, respectively. Biochemical disease-free survival rates in patients with stage T1c, T2a and T2b groups at 2 years were 89, 67% and 40% ($p=0.0817$). Biochemical disease-free survival rates in patients with Gleason scores of 2-4, 5-7 and 8-10 at 2 years were 88, 72% and 80% ($p=0.6539$). Biochemical disease-free survival rates in patients with serum PSA of less than 10 ng/ml and 10-20 ng/ml were 75% and 78% ($p=0.6152$). No viable tumor cells were noted in 68% of patients by postoperative prostate needle biopsy. Prostatic volume was decreased from 24.2 ml to 14.0 ml at 6 months after HIFU ($p<0.01$). No statistically significant differences were noted in International Prostate Symptom Score, maximum urinary flow rate and quality of life analysis with Functional Assessment of Cancer Therapy. HIFU therapy appears to be minimally invasive, efficacious and safe for patients with localized prostate cancer with pretreatment PSA levels less than 20 ng/ml.

(Hinyokika Kiyo **51** : 651-658, 2005)

Key words: Prostate cancer, High-intensity focused ultrasound, Minimally invasive surgery

INTRODUCTION

Prostate cancer is the most common malignancy in men and the second leading cause of death due to cancer in the United States[1]. Prostate cancer has been treated in various ways, depending on the severity of the condition, age of the patient, staging, Gleason score and serum prostate-specific antigen (PSA) level. Radical prostatectomy has long been regarded as appropriate therapy for patients with organ-confined prostate cancer. Despite excellent 5- to 10-year survival rates after radical prostatectomy for organ-confined disease, surgery is

associated with significant morbidity, including blood loss due to transfusion-related complications, erectile dysfunction in 30% to 70% of cases, and stress incontinence in up to 10% of patients[2,3]. In addition, surgical intervention is not typically considered for patients whose life expectancy is less than 10 years. Recently, a number of alternative less invasive treatments have been developed for patients with localized prostate cancer, either not appropriate for surgery or who do not want to risk the potential side effects of surgery. Three-dimensional conformal radiotherapy (3D-CRT), brachytherapy, intensity-modulated external beam radiotherapy, cryosurgical ablation of the prostate and laparoscopic radical prostatectomy have all been applied for the treatment of this group of patients[4–6]. However, in the event of treatment failure, these cannot be repeated and salvage radical prostatectomy is associated with a high morbidity rate[7].

High-intensity focused ultrasound (HIFU) delivers intense ultrasound energy with consequent heat destruction of tissue at a specific focal distance from the probe without damage to tissue in the path of the ultrasound beam[8]. HIFU non-invasively induces complete coagulative necrosis of a tumor without surgical exposure or insertion of instruments into the lesion. This advantage makes it one of the most attractive options for the localized treatment of tumors[9,10]. We report here a multicenter trial with 72 consecutive patients treated with HIFU for clinical stage T1c-2N0M0 localized prostate cancer.

PATIENTS AND METHODS

Inclusion and Exclusion Criteria

As a rule, the inclusion criteria for treatment were patients with biopsy proven and untreated stage T1c-2N0M0 localized prostate cancer[11]. Age, serum PSA levels, prostatic volume and WHO performance status should be less than 80 yrs, 20 ng/ml, treatable with a 4.0 focal length probe which means a prostatic volume less than 50 ml and 0–1. Patients with urethral stricture, anal stricture, bleeding tendency, renal dysfunction with serum Cr more than 2.0 mg/dl, hydronephrosis, larger than 5 mm calcifications in the prostate, uncontrolled diabetes mellitus, hypertension, angina, history of cardiac infarction or other malignant diseases were excluded from the study. None of the patients were receiving neoadjuvant hormonal and/or chemotherapy before HIFU. All patients were fully informed of the details of this treatment and gave written consent preoperatively.

HIFU Eqipment

For this study, we used the Sonablate 500™ (Focus Surgery, Indianapolis, IN, USA) HIFU machine. This treatment module includes the ultrasound power generator, transrectal probes, the probe positioning system, and a continuous cooling system (Fig. 1). The

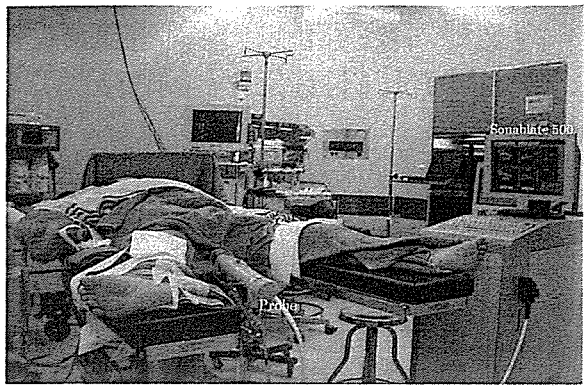

Fig. 1. The Sonablate-500™ type device consists of an operator's console, imaging monitor, transrectal probe and an automatic continuous cooling system.

transrectal HIFU probes use proprietary transducer technology with low-energy ultrasound (4 MHz) for imaging of the prostate and for the delivery of high-energy ablative pulses (site intensity, 1,300–2,200 W/cm^2). The single piezoelectric crystal alternates between high-energy power for ablative (3 sec) and low-energy for ultrasound imaging (6 sec)[10].

Prior to beginning the treatment, the operator uses longitudinal and transverse sonograms to obtain an image of the prostate and selects the prostate tissue volume to be ablated by a set of cursors on these images. The probe houses a computer-controlled positioning system that directs each ablative pulse to the targeted region of the prostate. Each discrete high-energy focused ultrasonic pulse ablates a volume of $3 \times 3 \times 10$ mm^3 of tissue[10]. The total acoustic power is initially set at 24 W and 37 W for 3.0 and 4.0 cm focal length probes, respectively. The individual focal lesion produces almost instantaneous coagulative necrosis of the tissue due to a temperature rise of 80° to 98°C in the focal zone[8]. Under computer control, the ultrasound beam is steered mechanically to produce consecutive lesions in a manner such that all focal lesions overlap

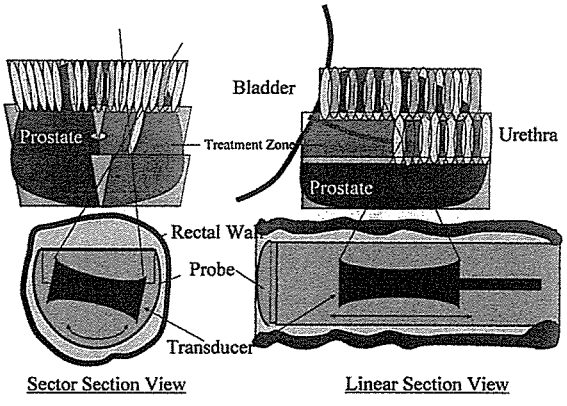

Fig. 2. The computer-controlled transducer ablates the entire prostate tissue. Focal lesions are overlapped in linear rows (left) at each of the lateral sector positions (right) to create a volume lesion.

laterally and longitudinally to ensure necrosis of the entire targeted prostate volume (Fig. 2). An automatic cooling device is used during treatment to maintain a constant baseline temperature of less than 18°C in the transrectal probe that helps to prevent thermal injury of the rectal mucosa.

HIFU Procedure

All patients were anesthetized by general, epidural, spinal or intravenous anesthesia, and were placed in a supine and open leg position. A condom was placed over the probe and degassed water was used to inflate the condom that was covered with ultrasound gel for close coupling of the ultrasound probe to the rectal wall, and the probe was inserted manually into the rectum. The probe was fixed in position by an articulating arm attached to the operating table. After selection of the treatment region of the prostate from the verumontanum to the bladder neck, the treatment was started. Transrectal probes with focal lengths of 3.0 and 4.0 cm were used according to the size of the prostate as determined by transrectal ultrasound (TRUS), with larger glands requiring longer focal lengths. The treatment continued layer by layer (10 mm thickness) from the apex to the base (Fig. 2). Usually, three successive target areas (anterior, mid-part and base) were defined to treat the whole prostate. After treatment was completed, a transurethral balloon catheter was inserted into the bladder[10].

Clinical Follow-up and Definition of Outcome

Patient status and treatment-related complications were followed up by all available means, including periodic patient visits and self-administered questionnaires dealing with urinary continence and erectile function using Functional Assessment of Cancer Therapy (FACT) questionnaire. Urinary symptoms and urinary flow rate analysis were performed using International Prostate Symptom Score (I-PSS) index and urowflowmetry[12,13]. Serum PSA was assayed every 1 to 6 months during follow-up. A postoperative prostate needle biopsy under TRUS was performed on all patients at 6 months. The American Society for Therapeutic Radiology and Oncology (ASTRO) consensus definition, i.e., three consecutive increases in post treatment PSA after a nadir has been achieved, was used to define biochemical failure[14]. The time to biochemical failure was defined as midway between the post treatment PSA nadir and the first of three consecutive PSA increases. None of the patients received androgen deprivation after HIFU or other anticancer therapy before documentation of a biochemical recurrence. HIFU related complications were defined by Japanese version of National Cancer Institute-Common Toxicity Criteria version 2.0[15].

Statistical Analyses

All statistical analyses were performed by the Department Statistics in Indiana University. The chi-square test was used to assess the correlation between preoperative and postoperative parameters. The distributions of biochemical disease-free survival times were calculated according to the Kaplan-Meier curves and the logrank test was used to compare curves for groups. All p values less than 0.05 reflected statistically significant differences.

RESULTS

A total of 75 patients were entered in the trial. The prostate was treated in 1 (75) or 2 (14) HIFU sessions in a total of 89 procedures (1.2 sessions/patient). One patient with stage T1b, 1 patient with a serum PSA of 20.60 ng/ml and 1 patient on whom treatment was stopped during the procedure because of appearance with large microbubbles in the prostate were excluded. The median age, serum PSA level and prostatic volume of the 72 patients analysed were 72 yrs (range 45 to 79), 8.10 ng/ml (range 2.10 to 19.80) and 22.1 ml (range 8.5 to 52.8), respectively. The TNM stage was T1c in 40 patients, T2a in 18 patients and T2b in 14 patients. All patients had a histological diagnosis of prostatic adenocarcinoma according to the Gleason grading system. The Gleason score was 2 to 4 in 9 patients, 5 to 7 in 55 patients, 8 to 10 in 6 patients and unknown in 2 patients (Table 1).

The median time of HIFU treatment and hospitalization was 169 min (range 65 to 485 min) and 5.0 days (range 2 to 55), respectively. The gland size decreased from an initial volume of 24.2 ml to a final median volume of 14.0 ml ($p < 0.01$) in 45 patients. Totally, 49 out of 72 (68%) had negative follow-up biopsies at 6 months after HIFU. Biochemical disease-free survival rates were analyzed in 60 patients. Twelve patients were excluded from the analysis for unsatisfactory followup. The median follow-up period for all patients was 14.0 months (range 2 to 24). Biochemical disease-free survival rates in all patients at 1

Table 1. Characteristics in 72 patients with localized prostate cancer

Median age (range)	72 (45–79)
Median PSA (range)	8.10 ng/ml (2.10–19.80)
Prostate volume (range)	22.1 (8.5–52.8)
Pretreatment PSA (%):	
10 or less	44 (61)
10.1–20	28 (39)
Clinical stage (%):	
T1c	40 (56)
T2a	18 (25)
T2b	14 (19)
Gleason score (%):	
2–4	9 (13)
5–7	55 (76)
8–10	6 (8)
Unknown	2 (3)
Median mos followup (range)	14.0 (2–24)

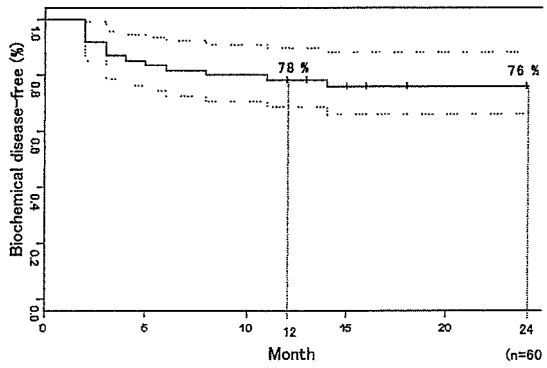

Fig. 3. Kaplan-Meier biochemical disease-free survival curves in all patients.

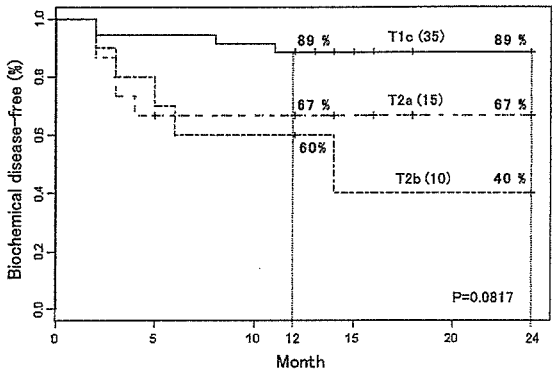

Fig. 4. Kaplan-Meier biochemical disease-free survival curves according to clinical stage.

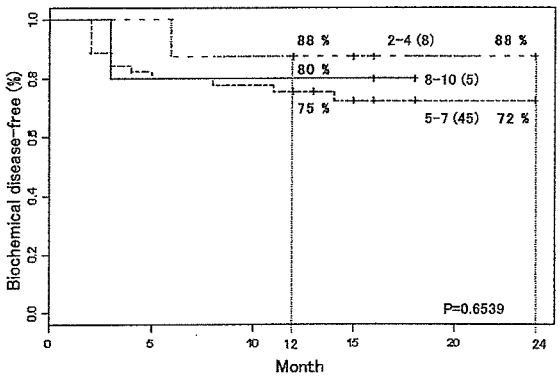

Fig. 5. Kaplan-Meier biochemical disease-free survival curves according to Gleason score.

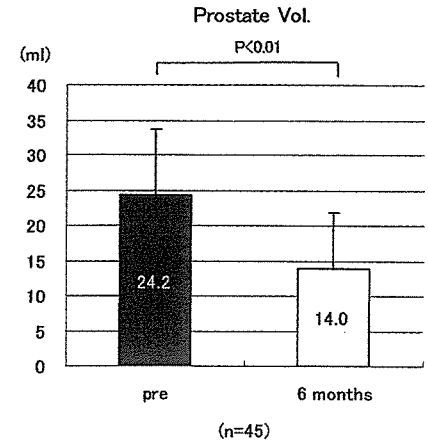

Fig. 6. Changes of prostatic volume.

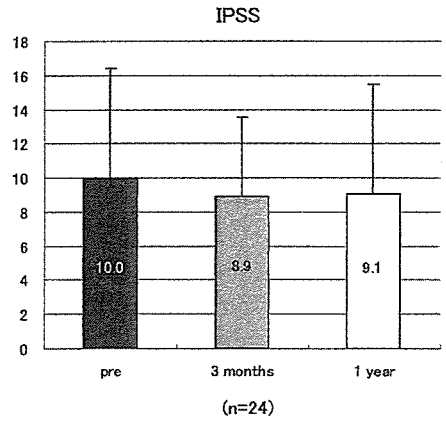

Fig. 7. Changes of International Prostatic Symptom Score.

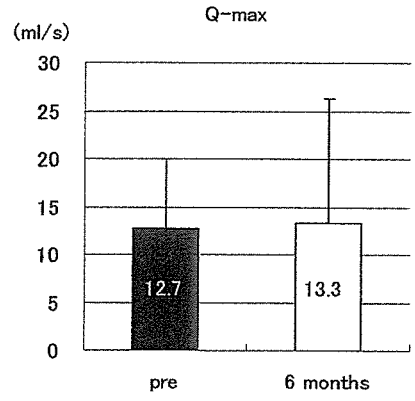

Fig. 8. Changes of maximum flow rate.

and 2 years were 78% and 76%, respectively (Fig. 3). Biochemical disease-free survival rates in patients with stage T1c, T2a and T2b groups at 2 years were 89%, 67% and 40% ($p = 0.0817$, Fig. 4). Biochemical disease-free survival rates in patients with Gleason 2–4, 5–7 and 8–10 groups at 2 years were 88, 72% and 80% ($p = 0.6539$, Fig. 5). The biochemical disease-free survival rate in patients whose serum PSA less than 10 ng/ml and 10 – 20 ng/ml were 75% and 78% ($p = 0.6152$).

Prostatic volume was decreased from 24.2 ml to 14.0 ml at 6 months after HIFU ($p < 0.01$, Fig. 6). No statistically significant difference was noted in I-PSS, Q-max and FACT quality of life analysis (Fig. 7, 8 and 9).

Thirteen out of 72 patients developed a urethral stricture, 6 and 4 patients developed epididymitis and prostatitis. Postoperative erectile dysfunction was noted in 12 out of 31 (39%) patients who were potent preoperatively. Nephrotic syndrome, transient urinary incontinence, transit stooly incontinence, balanoposthitis or retrograde ejaculation was observed in 1 patient each (Table 2).

For analysis of HIFU treatment using Sonablate 500^{TM}, ultrasound imaging for identifying prostate and quality levels were categorized more than good in patients with 92%. A transrectal probe was easily

Table 2. Complications

Complication	Grade 1	Grade 2	Grade 3	Grade 4	Total
Urethral stricture	0	0	13	0	13
Erectile dysfunction (31 potent patients)	0	0	12	0	12
Epididymitis	2	2	2	0	6
Prostatitis	2	0	2	0	4
Nephrotic syndrome	0	0	1	0	1
Balanoposthitis	1	0	0	0	1
Uninary incontinence (grade 1)	1	0	0	0	1
Stooly incontinence	1	0	0	0	1
Retograde ejaculation	1	0	0	0	1

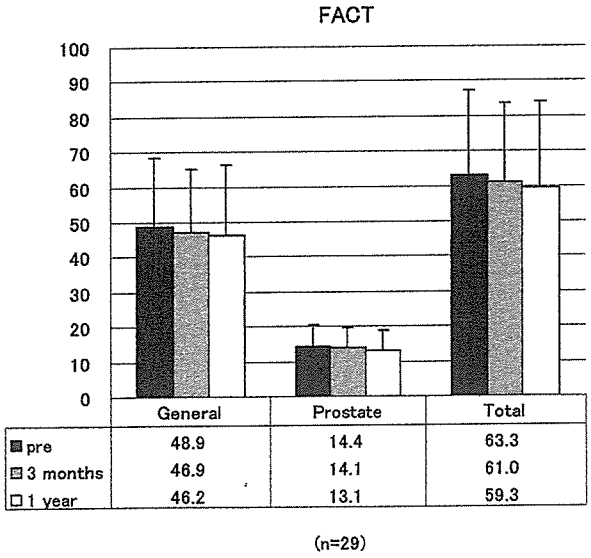

Fig. 9. Quality of life change by FACT general and prostate.

inserted into the rectum in 97% of the patients. Totally, 96% of the HIFU treatment was categorized as an easy procedure.

DISCUSSION

In 1995, Madersbacher et al. reported the effectiveness of HIFU in 10 cases of localized prostate cancer[8]. Histologically, HIFU-treated lesions of the prostate demonstrated a coagulation necrosis with sharp boundaries. In 1996, Gelet et al. reported preliminary experiences with HIFU using the Ablatherm device (EDAP-Technomed, Lyon, France) for treating localized prostate cancer[16]. Beerlage et al. reported the results of HIFU treatments in 111 patients with clinical stage T1-3N0M0 prostate cancer and a PSA level less than 25 ng/ml. The treatment for the first 49 patients was performed selectively (i.e. unilateral or bilateral treatment in one or two sessions depending on findings from TRUS and biopsies) and the whole prostate was treated in the remaining 62 patients. A complete response (defined as a PSA level < 4.0 ng/ml and a negative biopsy) was achieved in 60% of the whole prostate treated patients with and in 25% of selectively treated patients[17].

In 2001, Gelet et al. reported their long-term follow-up data in which a complete response was obtained in 66% of patients with no residual cancer (regardless of PSA levels) or no increases in PSA levels in three consecutive examinations with a PSA velocity < 0.75 ng/ml/year for patients with negative biopsies[18]. More recently, Chaussy and Thuroff summarized clinical outcomes by the ASTRO definition as 84.2% stability rate in the HIFU group and 80% rate in the combination with transurethral resection of the prostate (TURP) and HIFU group in 1 year[19]. In summarizing our clinical outcome using the ASTRO definition, the biochemically disease-free survival rate was 76% at 2 years follow-up. Patients with stage T1c, T2a and T2b showed resectively 89, 67% and 40% biochemical disease-free survival rates at 2 years follow-up ($p=0.0817$). The clinical outcome in our series of patients with preoperative PSA less than 20 ng/ml were comparable to the outcome of patients treated with radical prostatectomy[2,3].

In our series, postoperative urethral strictures at near verumontanum in the prostatic urethra occurred in 21% of the patients. Recently, TURP or bladder neck incision immediately before or after HIFU was found to reduce the treatment-related morbidity such as postoperative prolonged urinary retention, urinary catheterization time and urinary infection[20,21]. Neoadjuvant hormonal therapy also might be useful to reduce the volume of the prostate which can reduce the time of treatment and rate of morbidity. However, the upper limit of the gland volume is 50 ml even after reducing the size of the prostate with neoadjuvant androgen deprivation or TURP in our series. Generally, radicalism of prostate cancer and preservation of sexual function are always controversial because postoperative impotence depends on preservation of neuro-vascular bundles that sometimes includes tumor invasion. In our study, 39% of the patients exhibited erectile dysfunction after the HIFU therapy. One out of 12 patients who desired treatment for postoperative erectile dysfunction recovered with sildenafil citrate. We considered this rate to be lower than that compared to radical prostatectomy[2,3]. Further experience is required to confirm this important conclusion.

D'Amico et al. compared the outcome of a cohort

treated with 3D-CRT versus a matched cohort treated with brachytherapy plus external radiation therapy. The 5-year estimate of PSA failure-free survival rate after 3D-CRT alone was 45% and 67% when both radiation treatments were combined[22]. More recently, Kupelian et al. compared the biochemical disease-free survival rate after permanent seed brachytherapy, external beam radiation therapy (EBRT), combined seeds and EBRT, or radical prostatectomy for clinical stage T1-2 localized prostate cancer[23]. The 5-year biochemical disease-free survival rate for radical prostatectomy, EBRT <72 Gy, EBRT ≥ 72 Gy, permanent seed brachytherapy and combined seeds and EBRT were 81, 51, 81, 83% and 77%, respectively. Although not directly comparable, the results after treatment with HIFU appear to be similar to those after radiotherapy, even when both brachytherapy and EBRT are combined.

For many reasons, transrectal HIFU appears to be highly attractive as a minimally invasive treatment for localized prostate cancer. HIFU treatment requires no incision or puncture, with no bleeding, can be performed on an outpatient basis and is repeatable even when patients with local recurrence have already been treated with radiation therapy[24]. In addition, radiation therapy including brachytherapy and even surgery can be performed after HIFU.

Transrectal HIFU has considerable potential as a noninvasive treatment modality for patients with localized prostate cancer especially whose PSA less than 20 ng/ml.

ACKNOWLEGEMENTS

The authors express their appreciation to Mr. Y. Shimazaki, S. Kagosaki, K. Yamashita, K. Takai and N.T. Sanghvi for their technical assistance.

REFERENCES

1) Landis SH, Murray T, Bolden S, et al.: Cancer statistics, 1999. CA Cancer J Clin **49**: 8, 1999
2) Hull GW, Rabbani F, Abbas F, et al.: Cancer control with radical prostatectomy alone in 1,000 consecutive patients. J Urol **167**: 528–534, 2002
3) Roehl KA, Han M, Ramos CG, et al.: Cancer progression and survival rate following anatomical radical retropubic prostatectomy in 3,478 consecutive patients: long-term results. J Urol **172**: 910–914, 2004
4) Zelefsky MJ, Hollister T, Raben A, et al.: Five-year biochemical outcome and toxicity with transperineal CT-planned permanent I-125 prostate implantation for patients with localized prostate cancer. Int J Radiat Oncol Biol Phy **47**: 1261–1266, 2000
5) Guillonneau B, el-Fettouh H, Baumert H, et al.: Laparoscopic radical prostatectomy: oncological evaluation after 1,000 cases a Montsouris experience. J Urol **169**: 1261–1266, 2003
6) Han K-R, Cohen JK, Miller RJ, et al.: Treatment of organ confined prostate cancer with third generation cryosurgery: preliminary multicenter experience. J Urol **170**: 1126–1130, 2003
7) Lerner SE, Blute ML and Zinke H: Critical evaluation of salvage surgery for radio-recurrent/resistant prostate cancer. J Urol **154**: 1103–1109, 1995
8) Madersbacher S, Pedevilla M, Vingers L, et al.: Effect of high-intensity focused ultrasound on human prostate cancer in vivo. Cancer Res **55**: 3346–3351, 1995
9) Uchida T, Sanghvi NT, Gardner TA, et al.: Transrectal high-intensity focused ultrasound for treatment of patients with stageT1b-2N0M0 localized prostate cancer: a preliminary report. Urology **59**: 394–399, 2000
10) Uchida T, Tsumura H, Yamashita H, et al.: Transrectal high-intensity focused ultrasound for treatment of patients with stageT1b-2N0M0 localized prostate cancer: a preliminary report. Jpn J Endourol ESWL **16**: 108–114, 2003
11) Sobin LH and Wittekind CH: TNM classification of Malignant Tumors (5th ed). Wiley-Liss Inc, 1997
12) Cella DF, Tulsky DS, Gray G, et al.: The functional assessment of cancer therapy scale: development and validation of the general measure. J Clin Oncol **11**: 570–579, 1993
13) Japanese Urological Association and the Japanese Society of Pathology. General Rule for Clinical and Pathological Studies on Prostate Cancer. April 2001 (The 3rd edition). Tokyo, Kanehara Co
14) Consensus statement: Guidelines for PSA following radiation therapy. American Society for Therapeutic Radiology and Oncology Consensus Panel. Int J Radiat Oncol Biol Phys **37**: 1035–1041, 1997
15) National Cancer Institute-Common Toxicity Criteria. Version 2.0, April 30, 1999
16) Gelet A, Chaperon JY, Bouvier R, et al.: Treatment of prostate cancer with transrectal focused ultrasound: early clinical experience. Eur Urol **29**: 174-183, 1996
17) Beerlage HP, Thüroff S, Debruyne FMJ, et al.: Transrectal high-intensity focused ultrasound using the Ablatherm device in the treatment of localized prostate carcinoma. Urology **54**: 273–277, 1999
18) Gelet A, Chapelon JY, Bouvier R, et al.: Transrectal high-intensity focused ultrasound for the treatment of localized prostate cancer: factors influencing the outcome. Eur Urol **40**: 124–129, 2001
19) Chaussy CG and Thüroff S: The status of high-intensity focused ultrasound in the treatment of localized prostate cancer and the impact of a combined resection. Curr Urol Rep **4**: 248–252,

2003
20) Thüroff S, Chaussy C, Vallancien G, et al.: High-intensity focused ultrasound and localized prostate cancer: efficacy results from the European multicentric study. J Endourol **17**: 673–677, 2003
21) Vallancien G, Prapotnich D, Cathelineau Y, et al.: Transrectal focused ultrasound combined with transurethral resection of the prostate for the treatment of localized prostate cancer: feasibility study. J Urol **171**: 2265–2267, 2004
22) D'Amico AV, Schultz D, Schneider L, et al.: Comparing prostate specific antigen outcome after different types of radiotherapy management of clinically localized prostate cancer highlights the importance of controlling for established prognostic factors. J Urol **163**: 1797–1801, 2000
23) Kupelian PA, Potters L, Khuntia D, et al.: Radical prostatectomy, external beam radiotherapy <72 Gy, external beam radiotherapy ≥72 Gy, permanent seed implantation, or combines seed/external beam radiotherapy for stage T1–T2 prostate cancer. Int J Radiat Biol Phys **58**: 25–33, 2004
24) Gelet A, Chapelon JY, Poissonnier L, et al.: Local recurrence of prostate cancer after external beam radiotherapy: early experience of salvage therapy using high-intensity focused ultrasonography. Urology **63**: 625–629, 2004

(Received on March 17, 2005
Accepted on June 25, 2005)
(迅速掲載)

和文抄録

限局性前立腺癌に対する高密度焦点式超音波療法：多施設共同研究

内田 豊昭[1]，馬場 志郎[2]，入江 啓[2]，宋 成浩[2]
舛森 直哉[3]，塚本 泰司[3]，中津 裕臣[4]，藤元 博行[5]
垣添 忠生[5]，植田 健[6]，市川 智彦[6]，太田 信隆[7]
北村 唯一[7]，住友 誠[8]，早川 正道[8]，青柳貞一郎[9]
橘 政昭[9]，池田 龍介[10]，鈴木 孝治[10]，鶴 信雄[11]
鈴木 和雄[11]，大園誠一郎[11]，藤本 清秀[12]，平尾 佳彦[12]
門田 晃一[13]，那須 保友[13]，公文 裕巳[13]，西 一彦[14]
上田 昭一[14]，古賀 寛史[15]，内藤 誠二[15]

[1]東海大学八王子病院泌尿器科，[2]北里大学医学部泌尿器科
[3]札幌医科大学泌尿器科，[4]旭中央病院泌尿器科
[5]国立がんセンター泌尿器科，[6]千葉大学医学部泌尿器科
[7]東京大学医学部泌尿器科，[8]防衛医科大学泌尿器科
[9]東京医科大学泌尿器科，[10]金沢医科大学医学部泌尿器科
[11]浜松医科大学医学部泌尿器科，[12]奈良県立医科大学医学部泌尿器科
[13]岡山大学医学部泌尿器科，[14]熊本大学医学部泌尿器科
[15]九州大学医学部泌尿器科

限局性前立腺癌に対する高密度焦点式超音波療法の多施設共同研究の成績について報告する．対象は，stageT1-2N0M0 の72例の限局性前立腺癌で，治療にはソナブレート500 (Focus Surgery, IN, USA) を用いた．効果判定には，American Society for Therapeutics Radiology and Oncology の効果判定基準を用いた．症例の年齢中央値は72歳，血清 PSA 中央値は 8.10 n/ml であった．また，術後観察期間中央値は14.0カ月間であった．治療効果は，全体では1年78%，2年76%が非再発生存であった．浸潤度別に2年目の生化学的非再発生存率を集計したところ，stage T1c が89%，stage T2a 67%，stage T2b は40% (p=0.0817) であった．悪性度別では，Gleason 2～4群は88%，Gleason 5～7群は72%，Gleason 8～10群は80% (p=0.6539) であった．術前の血清 PSA 値別2年非再発生存率は，PSA が10 ng/ml 以下群は75%，10～20 ng/ml 群は78% (p=0.6152) であった．術後6カ月目の前立腺生検では68%において癌細胞は認められなかった．前立腺体積は，術前 24.2 ml から術後6カ月目 14.0 ml と縮小していた (p<0.01)．IPSS，最大尿流量率，Functional Assessment of Cancer Therapy (FACT) を用いた生活の質項目は術前後に有意な変化は認められなかった．高密度焦点式超音波療法は，術前血清 PSA 値が 20 ng/ml 以下の限局性前立腺癌に対して低侵襲性でかつ有用な治療法と思われる．

(泌尿紀要 **51**：651-658，2005)

A New Method for Isolating Colonocytes From Naturally Evacuated Feces and Its Clinical Application to Colorectal Cancer Diagnosis

HISAYUKI MATSUSHITA,* YASUHIRO MATSUMURA,* YOSHIHIRO MORIYA,† TAKAYUKI AKASU,† SHIN FUJITA,† SEIICHIRO YAMAMOTO,† SHIGEKI ONOUCHI,† NORIO SAITO,§ MASANORI SUGITO,§ MASAAKI ITO,§ TAKAHIRO KOZU,¶ TAKASHI MINOWA,‖ SAYURI NOMURA,‖ HIROYUKI TSUNODA,# and TADAO KAKIZOE**

*Investigative Treatment Division, Research Center for Innovative Oncology, National Cancer Center Hospital East, Kashiwa; †Department of Surgery, National Cancer Center Hospital, Tokyo; §Department of Surgery, National Cancer Center Hospital East, Kashiwa; ¶Cancer Screening Division, National Cancer Center Research Center for Cancer Prevention and Screening, Tokyo; ‖Hitachi, Ltd., Life Science Group, Saitama; #Hitachi, Ltd., Advanced Research Laboratory, Tokyo; and **National Cancer Center, Tokyo, Japan

Reprinted from
GASTROENTEROLOGY
Volume 129, Number 6, December 2005

GASTROENTEROLOGY 2005;129:1918–1927

A New Method for Isolating Colonocytes From Naturally Evacuated Feces and Its Clinical Application to Colorectal Cancer Diagnosis

HISAYUKI MATSUSHITA,* YASUHIRO MATSUMURA,* YOSHIHIRO MORIYA,† TAKAYUKI AKASU,† SHIN FUJITA,† SEIICHIRO YAMAMOTO,† SHIGEKI ONOUCHI,† NORIO SAITO,§ MASANORI SUGITO,§ MASAAKI ITO,§ TAKAHIRO KOZU,¶ TAKASHI MINOWA,‖ SAYURI NOMURA,‖ HIROYUKI TSUNODA,# and TADAO KAKIZOE**

*Investigative Treatment Division, Research Center for Innovative Oncology, National Cancer Center Hospital East, Kashiwa; †Department of Surgery, National Cancer Center Hospital, Tokyo; §Department of Surgery, National Cancer Center Hospital East, Kashiwa; ¶Cancer Screening Division, National Cancer Center Research Center for Cancer Prevention and Screening, Tokyo; ‖Hitachi, Ltd., Life Science Group, Saitama; #Hitachi, Ltd., Advanced Research Laboratory, Tokyo; and **National Cancer Center, Tokyo, Japan

Background & Aims: **The early detection of colorectal cancer is desired because this cancer can be cured surgically if diagnosed early. The purpose of the present study was to determine the feasibility of a new methodology for isolating colonocytes from naturally evacuated feces, followed by cytology or molecular biology of the colonocytes to detect colorectal cancer originating from any part of the colorectum.** ***Methods:*** **Several simulation studies were conducted to establish the optimal methods for retrieving colonocytes from any portion of feces. Colonocytes exfoliated into feces, which had been retrieved from 116 patients with colorectal cancer and 83 healthy volunteers, were analyzed. Part of the exfoliated colonocytes was examined cytologically, whereas the remainder was subjected to DNA analysis. The extracted DNA was examined for mutations of the APC, K-*ras*, and p53 genes using direct sequence analysis and was also subjected to microsatellite instability (MSI) analysis.** ***Results:*** **In the DNA analysis, the overall sensitivity and specificity were 71% (82 of 116) of patients with colorectal cancer and 88% (73 of 83) of healthy volunteers. The sensitivity for Dukes A and B was 72% (44 of 61). Furthermore, the sensitivity for cancers on the right side of the colon was 57% (20 of 35). The detection rate for genetic alterations using our methodology was 86% (80 of 93) when the analysis was limited to cases in which genetic alterations were present in the cancer tissue.** ***Conclusions:*** **We have developed a new methodology for isolating colonocytes from feces. The present study describes a promising procedure for future clinical evaluations and the early detection of colorectal cancers, including right-side colon cancer.**

Colorectal cancer is one of the most common malignancies worldwide. In Japan, colorectal cancer is the third and second leading cause of death from cancer in men and women, respectively.[1] However, colorectal cancer is curable by surgical resection if diagnosed at a sufficiently early stage. This incentive has prompted investigators to develop new methods enabling the early diagnosis of colorectal cancer and has led to the introduction of cancer screening programs in many countries. For mass cancer screenings, a simple, economic, and noninvasive method of cancer detection is desired. The Hemoccult test is currently used in many countries for this purpose.[2–6] However, this test is nonspecific and is not sufficiently sensitive to detect early stage colorectal cancer, although a higher sensitivity has been reported for advanced-stage colorectal cancer.[7] Radioimmunoassays using tumor markers, such as carcinoembryonic antigen, also are not suitable for the detection of early cancer, although such tests can be used to monitor patients for an increasing tumor burden or tumor recurrence. Diagnosis by barium enema study and fiberoptic colonoscopy is accurate but time-consuming, expensive, and invasive. Therefore, an urgent need exists to establish a sensitive, reliable, and noninvasive method for the detection of colorectal cancer at an early stage.

To date, several screening methods for colorectal cancer based on the detection of mutated DNA in feces have been reported.[8–20] These methods, however, are time-consuming and are not sufficiently sensitive. The major reason for this inaccuracy is the fact that

Abbreviations used in this paper: APC, adenomatous polyposis coli; MSI, microsatellite instability; OMIM, Online Mendelian Inheritance in Man.

0016-5085/05/$30.00
doi:10.1053/j.gastro.2005.10.007

nucleic acids in feces are derived from an enormous number and variety of bacteria and normal cells. Accordingly, the proportion of genes derived from cancer cells in feces is as low as 1%, at most.[9] This makes the application of gene-detecting methods difficult in clinical practice.

We previously reported that the expression of CD44 variants in exfoliated colonocytes isolated from feces according to the Percoll centrifugation method could serve as a noninvasive diagnostic marker for early colorectal cancer.[21] However, the repetition of the Percoll centrifugation method was found to distort the morphology of the exfoliated colonocytes. Accordingly, the sensitivity of this method also appeared to be unsatisfactory because of the low retrieval rate of the exfoliated colonocytes. Another study described a processing method that involved scraping or washing the stool's surface with a buffer to collect exfoliated colonocytes.[22] In the ascending colon, however, the feces remains unformed. Therefore, most cancer cells exfoliated from the walls of the ascending colon would be incorporated into the inner core of the feces during the course of its formation. Thus, recovering cancer cells that originated from the ascending colon might be difficult using methods that involve scraping or washing solid feces.

Under these circumstances, we succeeded in developing a new, very effective methodology that allows the simple isolation of exfoliated colonocytes from not only the surface but also the central portion of feces while maintaining the colonocytes' initial morphology. Currently, we are attempting to apply a molecular biologic tool to purified colonocytes exfoliated into feces to detect cells from early colorectal cancers, including right-side colon cancer.

Materials and Methods

Study Design

This was a prospective study conducted between December 2002 and August 2004. The study protocol was reviewed and approved by the Institutional Review Board of the National Cancer Center, Japan. Written informed consent was obtained from all patients and healthy volunteers. No modifications to the protocol procedures were made during the course of the study.

Study Population

A total of 116 patients with histologically confirmed colorectal cancer and 83 healthy volunteers were enrolled. The healthy volunteers consisted of 37 men and 46 women with no apparent abnormalities, such as adenoma or carcinoma (including hyperplastic polyps), found during a total colonoscopy performed at the National Cancer Center Research Center for Cancer Prevention and Screening. The median age of these volunteers was 58.4 years (range, 40–70 years). The characteristics of the patients and healthy volunteers are summarized in Table 1. All the patients with colorectal cancer had undergone surgical resection of their primary tumor at the National Cancer Center Hospital, Tsukiji, or at Hospital East, Kashiwa, Japan. The median age of the patients was 62.0 years (range, 32–82 years). There were 69 men and 47 women patients. The primary tumors were located in the following sites: rectum in 53 patients, sigmoid colon in 21 patients, descending colon in 7 patients, transverse colon in 6 patients, ascending colon in 23 patients, and cecum in 6 patients. The clinical stage of the patients according to Dukes' classification was as follows: Dukes' stage A in 30 patients, stage B in 31 patients, stage C in 53 patients, and stage D in 2 patients.

Table 1. Characteristics of Patients and Healthy Volunteers

Characteristic	Patient (N = 116)	Healthy volunteer (N = 83)
Age, *y*		
Mean	62.0	58.4
Range	32–82	40–70
Sex, no (%)		
Male	69 (59.5)	37 (44.6)
Female	47 (40.5)	46 (55.4)
DNA, ng/gram of stool		
Mean	570.8	175.3
Range	2.0–7462.8	0.2–1907.5
Tumor location, no (%)		
Cecum	6 (5.2)	
Ascending colon	23 (19.8)	
Transverse colon	6 (5.2)	
Descending colon	7 (6.0)	
Sigmoid colon	21 (18.1)	
Rectum	53 (45.7)	
Size, mm		
Mean	40.0	
Range	4.0–120.0	
Histology, no (%)		
W/D	55 (47.4)	
M/D	56 (48.3)	
P/D	2 (1.7)	
Mucinous carcinoma	2 (1.7)	
Carcinoid tumor	1 (0.9)	
Depth, no (%)		
T1	10 (8.6)	
T2	32 (27.6)	
T3	71 (61.2)	
T4	3 (2.6)	
Dukes' stage, no (%)		
A	30 (25.9)	
B	31 (26.7)	
C	53 (45.7)	
D	2 (1.7)	

W/D, Well-differentiated adenocarcinoma; M/D, moderately differentiated adenocarcinoma; P/D, poorly differentiated adenocarcinoma.

Stool Samples

Before surgical resection, stool samples were obtained from 116 patients with colorectal cancer. Stool sam-

ples were also obtained from 83 healthy volunteers a few weeks after they had undergone a total colonoscopy. Naturally evacuated feces from subjects who had not taken laxatives were used as stool samples. Each patient was instructed to evacuate into a polystyrene disposable tray (AS one, Osaka, Japan) measuring 5 × 10 cm in size at home and bring the sample to the reception counter at the outpatient clinic or the Cancer Prevention and Screening Center of the National Cancer Center. The samples were collected and transferred to a laboratory at which they were allowed to stand at room temperature. Preparation of the stool samples for examination was conducted within 1–6 hours after the evacuation.

Magnetic Beads

Dynabeads Epithelial Enrich are uniform, superparamagnetic, polystyrene beads (4.5-μm diameter) coated with a mouse IgG1 monoclonal antibody (mAb Ber-EP4) specific for the glycopolypeptide membrane antigen Ep-CAM, which is expressed on most normal and neoplastic human epithelial tissues (Dynal, Oslo, Norway). Ep-CAM is widely expressed in the highly proliferative cells of the intestinal epithelium, from the basal cells to cells throughout the crypts at the basolateral membranes, and only the apical membrane facing the lumen is negative. The development of adenomas has been reported to be associated with increased Ep-CAM expression, and Ep-CAM over expression (mAb GA733) has frequently been demonstrated in colorectal carcinomas.[23–25]

Simulation Studies

A series of simulation studies were conducted to establish the optimal conditions for retrieving HT-29 colorectal cancer cells from feces. Feces from healthy volunteers were divided into several portions, each of which was seeded with 100 μL HT-29 cells (1 × 10^6/approximately 5 g feces). The cells were retrieved under several different conditions as follows: use of a Hank's solution and 25 mmol/L Hepes buffer (pH 7.35); processed feces of 5, 10, or 30 g volume; filter with a pore size of 48, 96, 512, or 1000 μm; incubation of homogenized solution with magnetic beads at 4°C or room temperature; application of 20, 40, 80, 200, or 400 μL magnetic beads; incubation of homogenized solution with magnetic beads under gentle rolling at 15 rounds/minute in a mixer for 10, 20, 30, or 40 minutes; and the reaction time between the cell-magnetic bead complexes and a magnet on a shaking platform for 0, 2, 10, 20, 30, 40, 50, or 60 minutes. Finally, the cell retrieval rate calculated for the magnetic beads method under the conditions determined to be the most suitable for this simulation study was compared with that calculated for the Percoll centrifugation method. The retrieval rate was calculated by dividing the number of cells that bound to the retrieved beads by the number of cells initially added to the feces. The cells were counted using a NucleoCounter (ChemoMetec A/S, Allerød, Denmark).

Isolation of Exfoliated Cells From Feces

The procedure was conducted using the most suitable and optimal conditions determined by the simulation study (Figure 1). Approximately 5–10 g of naturally evacuated feces were used to isolate exfoliated cells. Feces were collected into Stomacher Lab Blender bags (Seward, Thetford, United Kingdom). The stool samples were homogenized with a buffer (200 mL) consisting of Hank's solution, 10% fetal bovine serum (FBS), and 25 mmol/L Hepes buffer (pH 7.35) at 200 rpm for 1 minute using a Stomacher (Seward). The homogenates were then filtered through a nylon filter (pore size, 512 μm), followed by division into 5 portions (40 mL each). Subsequently, 40 μL of magnetic beads were added to each homogenized solution portion, and the mixtures were incubated for 30 minutes under gentle rolling in a mixer at room temperature. The samples on the magnet were then incubated on a shaking platform for 15 minutes at room temperature. Colonocytes isolated from 5 tubes were smeared onto slides and then stained using the Papanicolaou method. The remainder of the samples was centrifuged, and the sediments were stored at −80°C until DNA extraction.

Extraction of DNA

Fresh tissue samples were obtained from the surgically resected specimens of 116 patients with colorectal cancer. The samples were snap frozen in liquid nitrogen within 20 minutes of their arrival at the pathologic specimen reception area and were stored in liquid nitrogen until analysis.

Genomic DNA was extracted from each tumor tissue specimen using a DNeasy kit (QIAGEN, Valencia, CA). Genomic DNA was also extracted from colonocytes isolated from feces using the SepaGene kit (Sanko-Junyaku, Tokyo, Japan).

Direct Sequence Analysis

Direct sequencing was conducted to identify mutations in the APC codon 1270–1594, in codons 12 and 13 of the K-*ras* gene, and in exons 5, 6, 7, and 8 of the p53 gene.

The PCR primers used in this study were as follows: APC (5′-AAACACCTCAAGTTCCAACCAC-3′, 5′-GGTAATTTTGAAGCAGTCTGGGC-3′); K-*ras* (5′-CTGGTGGAGTATTTGATAGTG-3′, 5′-CCCAAGGAAAGTAAAGTTC-3′); p53 exon 5 (5′-GCCGTCTTCCAGTTGCTTTAT-3′, 5′-CCAAATACTCCACACGCAAAT-3′); p53 exon 6 (5′-CATGAGCGCTGCTCAGATAG-3′, 5′-TGCACATCTCATGGGGTTATAG-3′); p53 exon 7 (5′-CTTGGGCCTGTGTTATCTCCTA-3′, 5′-AAGAAAACTGAGTGGGAGCAGT-3′); and p53 exon 8 (5′-ACCTCTTAACCTGTGGCTTC-3′, 5′-TACAACCAGGAGCCATTGTC-3′).

The sequence primers used in this study were as follows: APC (5′-CAAAAGGCTGCCACTTGCAAAG-3′, 5′-AAAATAAAGCACCTACTGCTG-3′, 5′-GAATCAGCCAGGCACAAAGC-3′); K-*ras* (5′-CTGGTGGAGTATTTGATAGTG-3′); p53 exon 5 (5′-CCAAATACTCCACACGCAAAT-3′); p53 exon 6 (5′-CATGAGCGCTGCTCAGATAG-3′); p53 exon 7 (5′-AAGAAAACTGAGTGGGAGCAGT-3′); and p53 exon 8 (5′-